Acta Pharmaceutica Sinica B 2021;11(9):2645–2654

Chinese Pharmaceutical Association
Institute of Materia Medica, Chinese Academy of Medical Sciences

Acta Pharmaceutica Sinica B

www.elsevier.com/locate/apsb
www.sciencedirect.com

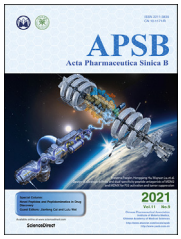

ORIGINAL ARTICLE

Peptidomimetic-based antibody surrogate for HER2

Mengmeng Zheng[a,†], Chunpu Li[a,b,c,†], Mi Zhou[a,†], Ru Jia[b], Fengyu She[a], Lulu Wei[a], Feng Cheng[d], Qi Li[b,c,*], Jianfeng Cai[a,*], Yan Wang[b,*]

[a]*Department of Chemistry, University of South Florida, Tampa, FL 33620, USA*
[b]*Department of Medical Oncology & Cancer Institute of Medicine, Shuguang Hospital, Shanghai University of Traditional Chinese Medicine, Shanghai 201203, China*
[c]*Academy of Integrative Medicine, Shanghai University of Traditional Chinese Medicine, Shanghai 201203, China*
[d]*Department of Pharmaceutical Science, College of Pharmacy, University of South Florida, Tampa, FL 33612, USA*

Received 16 March 2021; received in revised form 15 April 2021; accepted 20 April 2021

KEY WORDS

HER2;
Anti-cancer;
Peptidomimetics;
γ-AApeptides;
Antibody-surrogate

Abstract Inhibition of human epidermal growth factor receptor 2 mediated cell signaling pathway is an important therapeutic strategy for HER2-positive cancers. Although monoclonal antibodies are currently used as marketed drugs, their large molecular weight, high cost of production and susceptibility to proteolysis could be a hurdle for long-term application. In this study, we reported a strategy for the development of artificial antibody based on γ-AApeptides to target HER2 extracellular domain (ECD). To achieve this, we synthesized a one-bead-two-compound (OBTC) library containing 320,000 cyclic γ-AApeptides, from which we identified a γ-AApeptide, M-3-6, that tightly binds to HER2 selectively. Subsequently, we designed an antibody-like dimer of M-3-6, named M-3-6-D, which showed excellent binding affinity toward HER2 comparable to monoclonal antibodies. Intriguingly, M-3-6-D was completely resistant toward enzymatic degradation. In addition, it could effectively inhibit the phosphorylation of HER2, as well as the downstream signaling pathways of AKT and ERK. Furthermore, M-3-6-D also efficiently inhibited cell proliferation *in vitro*, and suppressed tumor growth in SKBR3 xenograft model *in vivo*, implying its therapeutic potential for the treatment of cancers. Its small molecular weight, antibody-like property, resistance to proteolysis, may enable it a new generation of artificial antibody surrogate. Furthermore, our strategy of artificial antibody surrogate based on dimers of cyclic γ-AApeptides could be applied to a myriad of disease-related receptor targets in future.

*Corresponding authors. Tel.: +86 21 20256517 (Qi Li), +1 813 9749506 (Jianfeng Cai), +86 21 20256533 (Yan Wang).
E-mail addresses: qili@shutcm.edu.cn (Qi Li), jianfengcai@usf.edu (Jianfeng Cai), yanwang@shutcm.edu.cn (Yan Wang).
[†]These authors made equal contributions to this work.
Peer review under responsibility of Chinese Pharmaceutical Association and Institute of Materia Medica, Chinese Academy of Medical Sciences.

https://doi.org/10.1016/j.apsb.2021.04.016

1. Introduction

HER2, also known as ERBB2, is a member of the human epidermal growth factor receptor family[1], and is associated with fundamental processes including tumor cell proliferation, apoptosis, adhesion, migration and differentiation[2–4]. Previous work has suggested that approximately 20% of breast cancers have genomic amplification or overexpression of this HER2 gene[5], therefore, HER2 is an important therapeutic target for the treatment of breast cancer.

Significant efforts have been extended to develop HER2-targeting drugs for treating HER2-positive breast cancer, including monoclonal antibodies (mAbs) trastuzumab[6] and pertuzumab[7] that bind to the extracellular domain of HER2 and small molecules tyrosine kinase inhibitors lapatinib[8] and neratinib[9] targeting intracellular kinase site. While these agents have significantly improved patient outcomes, there are still drawbacks associated with the treatment. For instance, the ultimate development of drugs resistance is common that presents a major challenge to the treatment of breast cancer in clinical therapy, particularly due to the use of tyrosine kinase inhibitors[10]. As to monoclonal antibodies, although they are highly specific, their high cost of production, large molecular weight, and susceptibility to enzymatic degradation, could be a hurdle for therapeutic development and long-term usage. In addition, recently clinical studies have suggested that the combinational treatment of HER2 inhibitors that inhibit HER2 by different mechanism is more effective than a single HER2 inhibitor. For example, the addition of tyrosine kinase inhibitors lapatinib showed improved activity in patients with monoclonal antibody trastuzumab treatment[11]. Treatment with monoclonal antibody trastuzumab and monoclonal antibody pertuzumab resulted in greater antitumor activity since trastuzumab binds to subdomain IV of the HER2 extracellular domain and pertuzumab binds HER2 at a different epitope of the HER2 extracellular domain (subdomain II)[12]. Furthermore, the triple combination of pertuzumab, trastuzumab and docetaxel significantly prolonged progression-free survival[13,14]. As such, there is continuing interest in the development of novel efficient HER2 targeting inhibitors which could either overcome the drawbacks of current therapeutic treatment or provide more combinational option needed on the success of HER2-targeted therapy.

Inspired by chiral PNA backbone, we recently developed a new class of peptidomimetics, γ-AApeptides[15,16] (Fig. 1), which could fold into well-defined protein-like helical structures stabilized by intramolecular hydrogen bond[17–20], providing a novel strategy to rationally design helical mimetics of important protein domain for protein surface recognition as well as disrupt critical protein−protein interactions[21]. Meanwhile, the unique γ-AApeptides backbone also provides a novel platform with remarkable stability and diversity that has been used to develop combinatorial libraries, from which unnatural ligands could be identified to bind to proteins or nucleic acids with high specificity and affinity[22–24]. In the current study, we report a strategy to develop new generation of artificial antibody based on γ-AApeptides. Dimerization strategy has been widely used to enhance the binding affinity of ligands toward protein targets, so as to develop unnatural antibody surrogate[25–29]. It is known that antibody contains two identical binding domains on the arms of the "Y" shape (Fig. 2B), each of which is a pseudo-loop formed by the heavy chain and the light chain. The divalent mode of antibody significantly enhances it binding affinity toward target molecules. We therefore proposed to identify cyclic γ-AApeptides that could target HER2 extracellular domain (ECD), and such molecules could mimic one binding loop of antibody. After such cyclic γ-AApeptides are linked by a bidentate linker, the newly obtained dimeric cyclic γ-AApeptides could theoretically mimic the function of antibody (Fig. 2B). As the molecular weight is much smaller than antibody, and γ-AApeptides are resistant to proteolysis, we could obtain novel peptidomimetic-based artificial antibody targeting HER2. To this end, to identify a new HER2 inhibitor, we developed a one-bead-two-compounds (OBTC) combinatorial library based on cyclic γ-AApeptides, and from which we identified a γ-AApeptide M-3-6 that exhibited high selectivity and excellent binding affinity to HER2. Subsequently, we designed an antibody-like dimer of M-3-6, M-3-6-D, which exhibited remarkable binding affinity to HER2 ECD. Intriguingly, both M-3-6 and M-3-6-D could effectively inhibit cell proliferation, coincided with down-regulation of phosphorylation on HER2 and their downstream signaling pathways including AKT and ERK. As anticipated, M-3-6-D showed a much better biological activity than M-3-6. Additionally, xenograft studies with SKBR3 breast cancer cells in mice demonstrated that M-3-6-D could significantly inhibit the tumor growth, with efficiency virtually identical to the marketed monoclonal drug trastuzumab.

2. Results and discussion

2.1. Library synthesis and screening

The OBTC combinatorial library was synthesized as reported previously[22] using peptide couplings and the sulfur-mediated SN2 reaction employed to construct thioether bridge for the cyclic γ-AApeptides. Briefly, each TentaGel bead was spatially segregated in two layers, which incorporate a cyclic γ-AApeptides on the surface layer and a linear α-peptides tag on the inner layer (Fig. 3A). The 320,000-member library which were displayed in triple that featured diversity at two positions in both side chains of every γ-AApeptide building block: the chiral side chains (R_1 in Fig. 3A) and the achiral side chains (R_2 in Fig. 3A) introduced by acylating the secondary amino group on the backbone. In addition,

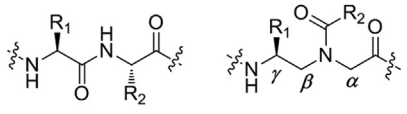

Figure 1 General structure of α-peptide and L-γ-AApeptide.

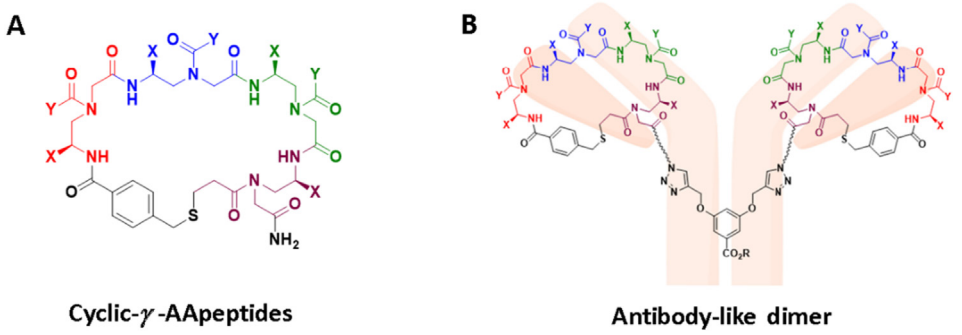

Figure 2 (A) Structure of the cyclic-γ-AApeptides and (B) artificial antibody based on cyclic-γ-AApeptides.

the linear decoding tag consisted of seven α-amino acid residues which were uniquely related to each side chain of the γ-AApeptides and were used for encoding the structure of the cyclic γ-AApeptides. The synthetic route is shown in Fig. 3B and details for library synthesis are provided in the Supporting Information.

After synthesis, the linear decoding tag of ten randomly selected beads were cleaved off by treatment with CNBr and subsequently analyzed by MALDI-TOF MS/MS. The result showed that eight beads had unambiguous MS/MS fragmentation patterns, suggesting the quality of the beads was excellent. Subsequently, the high-throughput screening for the HER2 protein was directly performed with the library using the protocol detailed in the Supporting information[22–24]. Briefly, to avoid the nonspecific binding and to improve the screening efficiency, prescreening

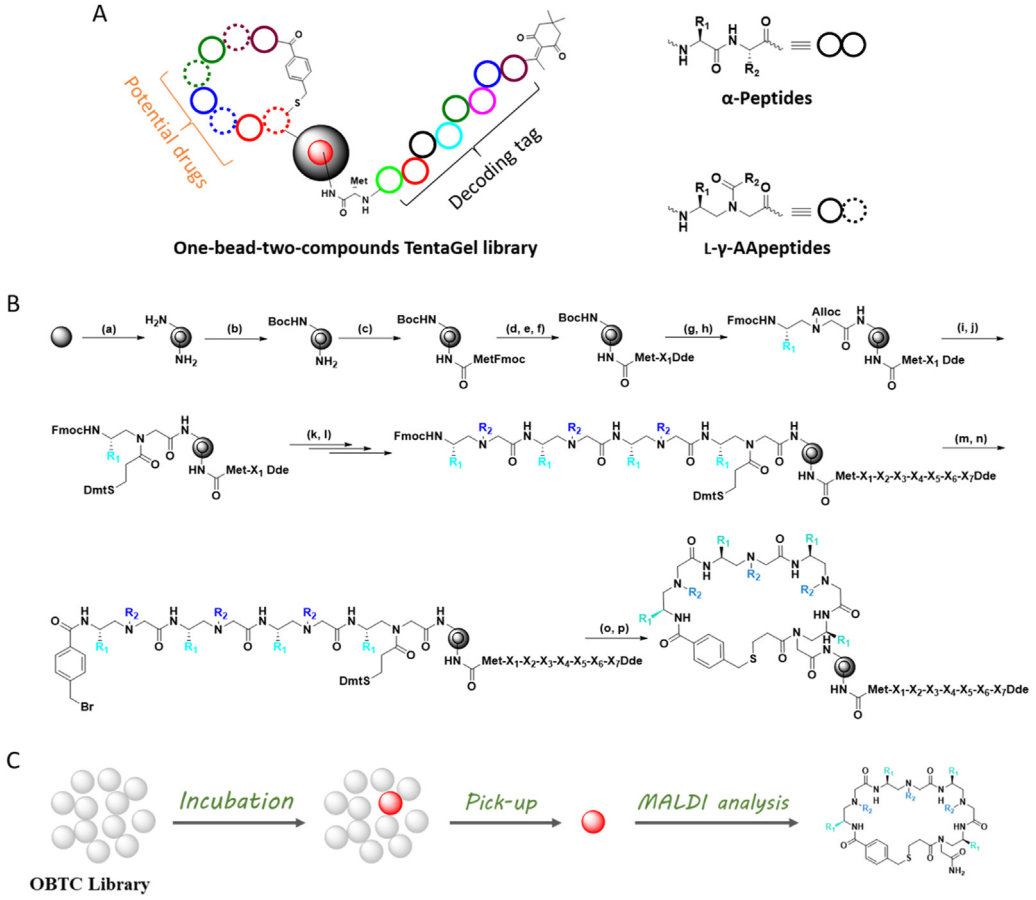

Figure 3 (A) Schematic presentation of one-bead-two-compounds TentalGel beads for library. (B) Scheme for the synthesis of OBTC cyclic γ-AApeptides library. (a) Soak in water for overnight; (b) $(Boc)_2O$, DCM/ether; (c) Fmoc-Met-OH, HOBt, DIC, DMF; (d) deprotect Fmoc by 20% piperidine in DMF; (e) split into five portions equally; (f) Dde protected amino acids, PyBOP, NEM, DMF; (g) deprotect Boc by TFA/triisopropylsilane/H_2O/Thioanisole (94:2:2:2); (h) Fmoc protected γ-AApeptides, HOBt, DIC, DMF; (i) deprotecting alloc by $Pd(PPh_3)_4$ and $Me_2NH{\cdot}BH_3$ in DCM; (j) Dmt protected mercaptopropionic acid, HOBt, DIC, DMF; (k) deprotecting Dde by $NH_2OH{\cdot}HCl$ and imidazole in NMP/DCM (5:1); (l) split-and-pool synthesis, repeating the previous steps; (m) deprotecting Fmoc by 20% piperidine in DMF; (n) 4-(bromomethyl)benzoyl chloride, DIPEA, DCM; (o) deprotecting Dmt by TFA/triisopropylsilane/DCM (2:2:96); (p) $(NH_4)_2CO_3$, DMF/H_2O (1:1). Xs are regular α-amino acids. (C) Scheme showing the overall strategy involved in library screening against HER2.

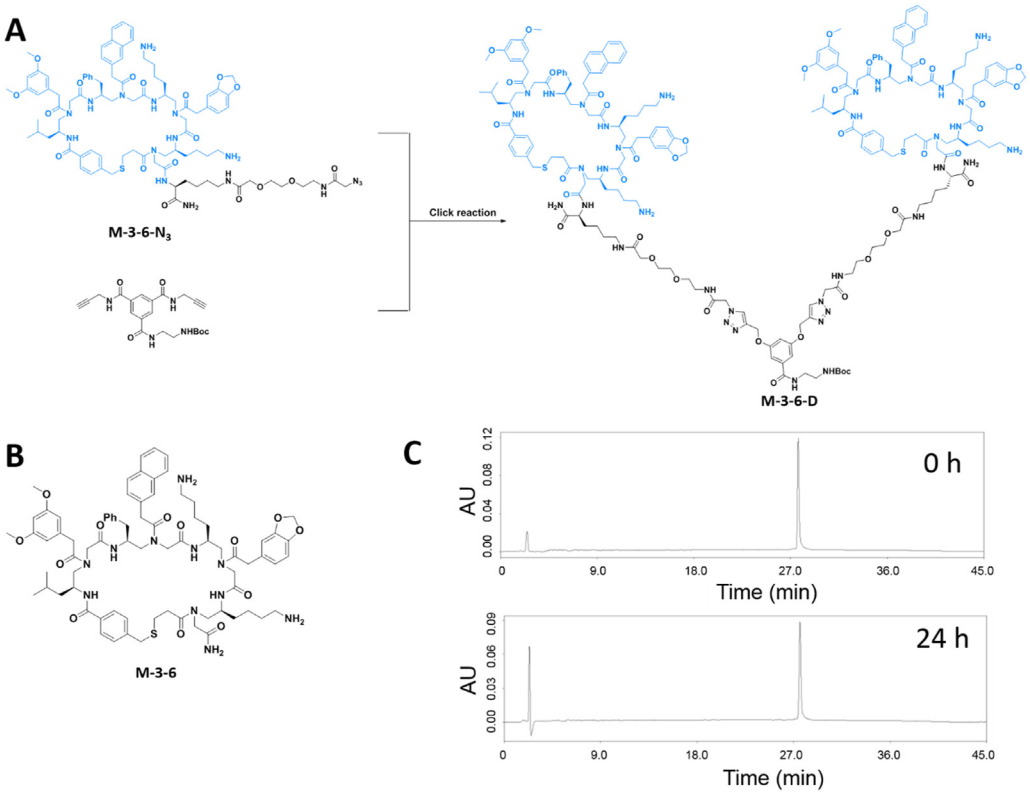

Figure 4 (A) The design and synthesis of M-3-6-D. (B) Chemical structure of cyclic γ-AApeptide M-3-6. (C) HPLC analytical trace of M-3-6-D after incubation with pronase (0.1 mg/mL) in 100 mmol/L ammonium bicarbonate buffer at 37 °C for 24 h.

was firstly performed, then the OBTC library was incubated with Fc-Tagged recombinant HER2 protein, followed by incubation with Goat anti-human IgG Fc cross adsorbed secondary antibody labeled with dylight 549 (Fig. 3B). After a thorough wash, six beads that emitting intensive red fluorescence (Supporting Information Fig. S1) were isolated from the library under a fluorescence microscope. These beads were treated with guanidium chloride (GdmCl) and then the linear encoding peptides in the inner layers of the beads were cleaved off and subsequently sequenced by tandem MS/MS of MALDI (Fig. 3B). As a result, all putative hits were determined unambiguously. Then fluorescein labeled putative hits (Supporting Information Fig. S2) were resynthesized on a larger scale individually and test for their ability to bind to HER2 *in vitro* by fluorescence polarization (FP) assay. Among them, one hit M-3-6-F exhibited strong binding affinity toward HER2 with a K_D of 0.28 μmol/L (Supporting Information Fig. S3).

2.2. *Design and synthesis of artificial antibody surrogate M-3-6-D*

The strong binding affinity of M-3-6 (Fig. 4B) prompted us to move forward for the design of γ-AApeptides based artificial antibody. Dimerization strategy has been widely used to enhance the binding affinity of ligands toward protein targets, so as to develop unnatural antibody surrogate[25−29]. Using the similar strategy, since M-3-6 could mimic a binding loop domain of the "Y" shaped monoclonal antibody (Fig. 2B), we could make a dimer of M-3-6 using a linker so as to mimic the two binding loop domains of antibody. As shown in Fig. 4A, an antibody-like dimer of M-3-6 could be designed in a very straightforward manner, which took advantage of the alkyne−azide click reaction with high reactivity for dimerization. Briefly, azide modified cyclic γ-AApeptide M-3-6-N_3 bearing a PEG linker to improve the solubility was synthesized on solid phase synthesis and then purified by HPLC, which could be dimerized with di-alkyne linker by click reaction to form M-3-6-D (Fig. 4A) that could possess the similar function as antibody. It should be noted that the length of PEG linker could be changed, thereby making it easily accessible to further optimize and enhance binding activity of this class of artificial antibody in the future.

2.3. *Binding affinity of M-3-6, M-3-6-D*

Next, the binding affinity of both M-3-6 and M-3-6-D to HER2 ECD *in vitro* were measured by surface plasmon resonance (SPR) assay (Supporting Information Fig. S4). M-3-6 shows a strong binding affinity to HER2 with a K_D of 228 nmol/L, which is highly consistent with the FP assay. As anticipated, the proposed artificial antibody, M-3-6-D, exhibited an excellent binding affinity toward HER2 with a K_D of 30 nmol/L, which has a ∼7-fold improvement of binding compared with monomer M-3-6, demonstrating the strategy of novel antibody-like design. In addition, EGFR, known as ERBB1, another member of the human epidermal growth factor receptor family was chosen to test the selectivity of M-3-6. The SPR assay shows that M-3-6 exhibited a 10-fold weaker binding to EGFR with a K_D of 1.95 μmol/L, demonstrating the good binding selectivity of M-3-6 to HER2 (Supporting Information Fig. S5).

2.4. *Stability of M-3-6-D toward proteolysis*

As M-3-6-D shows strong binding ability to HER2 *in vitro*, we further evaluated its proteolysis stability toward pronase (the

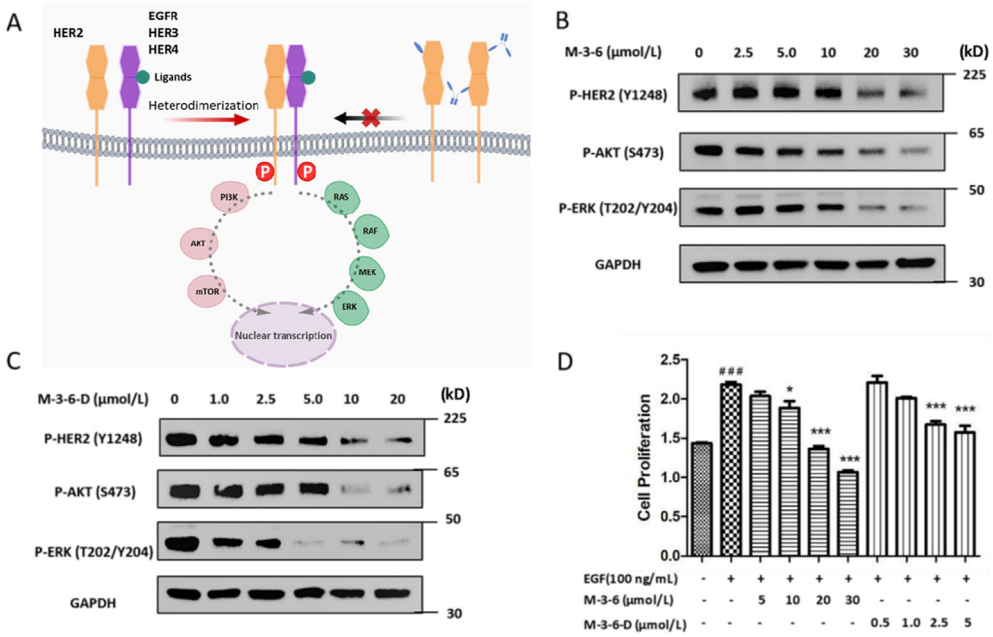

Figure 5 (A) Signal transduction pathway mediated by HER2 and proposed inhibition by cyclic peptides monomer and dimer. (B) Western blot analyses of SKBR3 cell lysates following M-3-6 incubation *in vitro*. M-3-6 treatment resulted in a dose-dependent inhibition of HER2 receptor phosphorylation and a reduction in the phosphorylation of AKT and ERK, downstream signaling of HER2. (C) Western blot analyses of SKBR3 cell lysates following M-3-6-D incubation *in vitro*. M-3-6-D treatment resulted in a much more effective phosphorylation inhibition compared with M-3-6. (D) M-3-6 and M-3-6-D inhibit cell proliferation. EGF-driven proliferation of SKBR3 cells was analyzed by CCK-8 proliferation assay. EGF (100 ng/mL) induced the proliferation of cells under serum-starved conditions ($^{###}P < 0.001$ *vs*. non-stimulated cells), and both M-3-6 and M-3-6-D inhibited EGF-induced proliferation significantly in a dose-dependent manner ($^{*}P < 0.05$ *vs*. EGF-stimulated cells, $^{***}P < 0.001$ *vs*. EGF-stimulated cells).

pronase theoretically digesting peptides into single amino acids) in buffer, which is critical for their biological activity. Upon incubation with pronase in 100 mmol/L ammonium bicarbonate buffer at 37 °C for 24 h, no detectable degradation was observed for M-3-6-D monitored by HPLC (Fig. 4C), demonstrating its extraordinary stability against proteolytic degradation.

2.5. *Inhibition of HER2, AKT, ERK phosphorylation in vitro*

Having confirmed the binding activity *in vitro*, we set out to test the monomer M-3-6 and antibody-like M-3-6-D for their ability to modulate HER2-mediated signaling pathways in cellular assays. Unlike HER1, HER3 and HER4, which interact with specific sets of ligands, HER2 has no known direct activating ligand but instead is constitutively able to activate by heterodimerization with other ligand-activated family members such as HER1 and HER3[4,30]. Upon heterodimerization, conformational changes lead to autophosphorylation and initiation of divergent signal transduction cascades, and the PI3K/AKT axis and the RAF/MAPK cascade are the two most important and most extensively studied downstream signaling pathways that are activated by the HER receptors[31−33]. Our cyclic γ-AApeptides, especially for our antibody-like M-3-6-D, which have potent binding affinity to HER2 ECD and may have the ability to inhibit HER2 heterodimerization (Fig. 5A), thereby inhibiting phosphorylation and downstream signal transduction.

As such, HER2-positive SKBR3 cells[34] were incubated with M-3-6 or M-3-6-D for 4 h and cell lysates were analyzed by western blotting. As shown in Fig. 5B, treatment of SKBR3 cells with M-3-6 (0−30 μmol/L) for 4 h resulted in a concentration-dependent inhibition of HER2 phosphorylation with an IC_{50} of 12.9 μmol/L, suggesting the compound blocked HER2 heterodimerization. Furthermore, downstream activation of phosphorylation of both AKT and ERK were also inhibited by M-3-6 *in vitro* with the consistent potency (IC_{50} for P-AKT is 16.9 μmol/L; and IC_{50} for P-ERK is 10.6 μmol/L) in a dose-dependent manner. As expected, the antibody-like molecule M-3-6-D showed even stronger inhibition of phosphorylation than M-3-6, which is in agreement with their binding affinity to HER2. As shown in Fig. 5C, the expression of P-HER2 was almost complete blocked with the treatment of 10 μmol/L M-3-6-D, while the expression of P-HER2 was relatively high with the incubation of M-3-6 at the same concentration (Fig. 5B). In addition, for the regulation of downstream signaling pathways, it is very interesting that M-3-6-D showed more pronounced effect on the suppression of P-ERK compared with P-AKT, which may be provide mechanistic insight into the HER2 mediated cell signaling. Together, these data indicated that both M-3-6 and M-3-6-D are potent inhibitors of HER2 and its downstream signaling pathways, and M-3-6-D demonstrated considerably higher efficiency which confirmed the antibody-like dimer design strategy.

2.6. *M-3-6, M-3-6-D inhibited cell proliferation in vitro*

Cell proliferation assay was subsequently carried out to further analyzed the effect of both M-3-6 and M-3-6-D on EGF-driven proliferation of SKBR3 cells *in vitro*, which is an important outcome of tumorigenesis. SKBR3 cells were treated with serum-reduced EGF-containing (100 ng/mL) McCoy's 5A Medium in the presence of M-3-6 and M-3-6-D at different concentration (0−30 μmol/L) for 72 h. As shown in Fig. 5D, SKBR3 cells showed

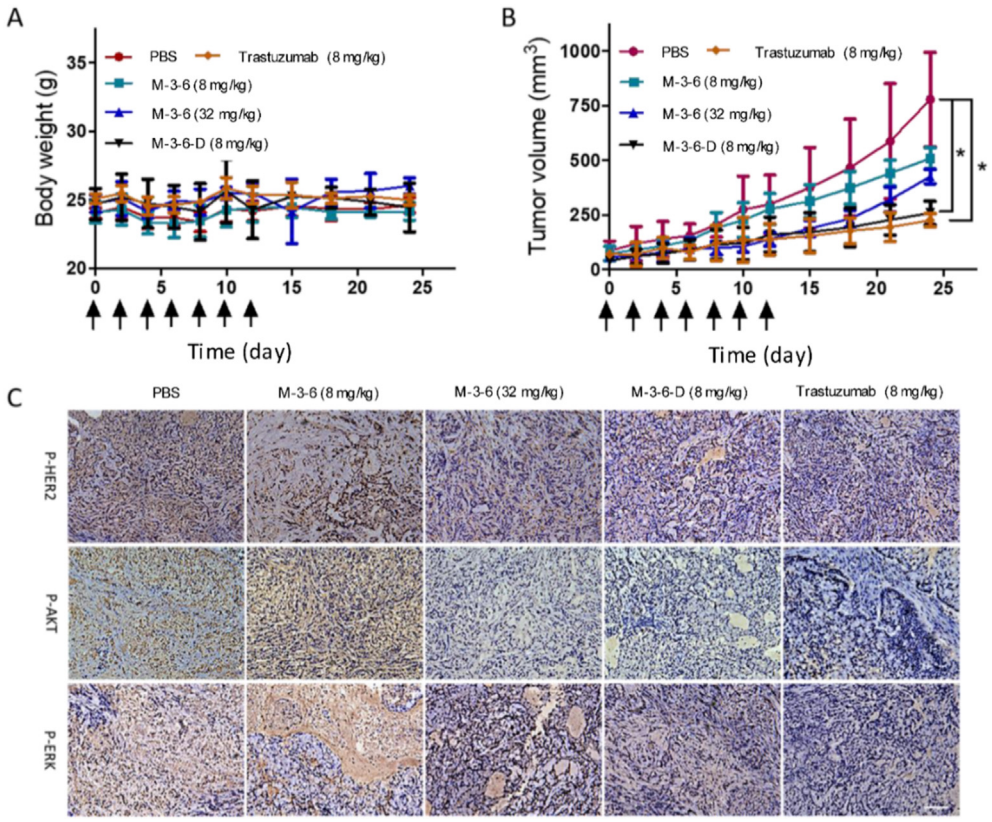

Figure 6 Therapeutic efficacy of M-3-6 and M-3-6-D in SKBR3 xenograft models. (A) Mice body weight shift curve of the mice during the experiment. Arrows indicate the time of compounds treatment. (B) Time course assessment of total tumor volume. The day when treatment started was recorded as day 0 and arrows indicate the time of injection. After 2 weeks injection, tumor volume was measured once every 3 days until Day 24. (C) Immunohistochemical staining for P-HER2, P-AKT and P-ERK. Representative staining of section from SKBR3 tumors with antibodies against the indicated proteins. Scale bar: 100 nm.

significantly enhanced proliferation upon the stimulation of EGF, in contrast, a significantly antiproliferative activity of M-3-6 on EGF-stimulated cells was observed in a dose-dependent manner with an IC_{50} of 17.9 μmol/L. It is intriguing that again M-3-6-D exhibited much stronger suppression of cells growth (IC_{50} is 1.66 μmol/L), which illustrated its therapeutic potential as novel anticancer agent.

2.7. The short-term therapeutic efficacy of M-3-6 and M-3-6-D in vivo

To further assess the potential of the new compounds as anticancer therapeutics, we evaluated the antitumor activity of both M-3-6 and M-3-6-D in a SKBR3 xenograft mouse model. The SKBR3 tumor xenograft mice were administrated with PBS (control), M-3-6 (8 or 32 mg/kg), M-3-6-D (8 mg/kg) or trastuzumab (8 mg/kg) by intraperitoneal (i.p.) injection respectively every two days for two weeks. The mice were allowed to grow for another 12 days before sacrifice. As shown in Fig. 6A, the injection of M-3-6 or M-3-6-D has ignorable effect on the body weight gain of SKBR3 tumor xenograft mice, indicating they negligible systematic cytotoxicity. The tumor size was measured with calipers showed extensive growth of the PBS-treated tumor. Though no significant reduction in tumor volume was observed of 8 mg/kg M-3-6 treatment, M-3-6 in higher dose (32 mg/kg) showed a much more improved antitumor effect, particularly in the period of drug administration. In comparison, antibody-like molecule M-3-6-D showed a significant antitumor effect, which is very comparable to that of the marketed monoclonal antibody Trastuzumab in the same concentration (Fig. 6B). It should be noted that after the last drug injection on Day 12, the significant reduction in tumor volume was still observed for trastuzumab and antibody-like M-3-6-D, suggesting that M-3-6-D exhibited antibody-like prolonged anticancer activity. On the contrary, a significant tumor growth was found between the PBS group and M-3-6 treatment, which may suggest binding affinity of ligands is crucial for continuous anticancer therapeutic effect. Subsequently, after mice were sacrificed, tumors were resected, and the phosphorylation level of HER2 in the SKBR3 tumor sections was analyzed by immunohistochemical staining. As shown in Fig. 6C, consistent to tumor volume, M-3-6 showed modest inhibitory effect, but antibody-like molecule M-3-6-D has comparable efficiency with trastuzumab. Taken together, these data show that M-3-6-D exhibits similar antitumor effectiveness compared to trastuzumab in SKBR3 xenografted model, which could be further investigated for promising clinical anti-cancer drug development.

3. Conclusions

We reported the development of novel artificial antibody by using a proper linker to dimerize two cyclic γ-AApeptides, so as to mimic both binding loops of monoclonal antibody. We demonstrated this strategy by identifying a novel HER2 inhibitor, cyclic

γ-AApeptide M-3-6 through an OBTC combinatorial library screening, which could bind toward HER2 with high affinity and selectivity, and inhibited HER2-mediated phosphorylation and downstream signaling transduction. The dimerization of M-3-6 using a properly designed linker led to an antibody-like molecule M-3-6-D, which showed remarkable binding affinity to HER2. This artificial antibody M-3-6-D could potently inhibit HER2 phosphorylation and downstream signal transduction, as well as suppressing cell proliferation. More importantly, M-3-6-D also demonstrated a similar robust antitumor activity to mAb Trastuzumab in tumor xenografts. With the small molecular weight, remarkable resistance to proteolysis, as well as antibody-like property, M-3-6-D could be a promising candidate for the development of novel antibody surrogate for the new generation of anticancer therapeutics. Moreover, our strategy of artificial antibody surrogate based on dimers of cyclic peptidomimetics could be applied to a myriad of disease-related receptor targets in future.

4. Experimental

All chemicals were purchased from commercial suppliers and used without further purification. Fmoc-protected amino acids were purchased from Chem-impex. TentaGel resin (0.23 mmol/g) was purchased from RAPP Polymere. Rink Amide-MBHA resin (0.55 mmol/g) was purchased from GL Biochem. Solid phase synthesis was conducted in peptide synthesis vessels on a Burrell Wrist-Action shaker. Cyclic γ-AApeptides were analyzed and purified on a Waters Breeze 2 HPLC system, and then lyophilized on a Labcono lyophilizer. The purity of the compounds was determined to be >95% by analytical HPLC. Masses of γ-AApeptides and the MS/MS analysis were obtained on an Applied Biosystems 4700 Proteomics Analyzer.

The SKBR3 cell lines were kindly provided by Prof. Lixin Wan at the Moffitt Cancer Center, Tampa, USA. HER2 was purchased from Creative BioMart; Anti-phospho-HER2 antibody was purchased from Thermo Fisher Scientific; Anti-phospho-AKT and Anti-phospho-ERK antibodies were from Cell Signaling Technology; GAPDH loading control monoclonal antibody was purchased from Invitrogen.

4.1. *One-bead-two-compound library synthesis, screening and analysis*

The one-bead-two-compound library was synthesized as our previous work[22]. 6.26 g TentaGel NH_2 resin was used for the library synthesis. The building blocks, side chains, linkers and Dde-protected amino acids that were used in this library were shown in Supporting Information Scheme S1.

For the HER2 targeted library screening, it contains two main parts, prescreening and screening.

Firstly, for the prescreening, all the TentaGel beads were swelled in DMF for 1 h. After being washed with Tris buffer for five times, the beads were equilibrated in Tris buffer overnight at room temperature, followed by incubation with the blocking buffer (1% BSA in Tris buffer with a 1000× excess of cleared *E. coli* lysate) for 1 h. After a thorough wash with Tris buffer, the beads were incubated with Goat anti-human IgG His cross adsorbed secondary antibody-dylight 549 (1:1000 dilution) for 2 h at room temperature. The beads were washed with the Tris buffer for five times and then the beads emitting red fluorescence were picked up manually and excluded from formal screening.

Secondly, for the screening, the rest of beads after prescreening were washed with Tris buffer, and treated with 8 M guandine·HCl at room temperature for 1 h, followed by wash with DI water (5×), tris buffer (5×) and DMF (5×). The beads were then incubated in DMF for 1 h, followed by washing and equilibration in Tris buffer overnight. The beads were incubated in 1% BSA/Tris buffer and 1000× excess of *E. coli* lysate for 1 h at room temperature. After wash with Tris buffer for five times, the beads were incubated with HER2 protein at a concentration of 50 nmol/L for 4 h at room temperature with a 1000× excess of *E. coli* lysate. After the thorough wash with Tris buffer, the library beads were incubated with and goat anti-human IgG Fc cross adsorbed secondary antibody-dylight 549 (1:1000 dilution) for 2 h at room temperature. The beads were washed with the Tris buffer for five times and then the beads emitting red fluorescence were picked up for future analysis.

For the hit structure analysis, each putative hit was transferred to an Eppendorf microtube, and denatured in 100 μL 8 mol/L guanidine·HCl for 1 h at room temperature respectively. The bead was rinsed with Tris buffer 3 × 10 min, water 3 × 10 min, DMF 3 × 10 min, and ACN 3 × 10 min. At last the resin was placed in ACN overnight in each microtube and then ACN was evaporated. The bead was incubated in the cocktail of 5:4:1 (*v*/*v*/*v*) of ACN: glacial acetic acid: H_2O containing cyanogen bromide (CNBr) at a concentration of 50 mg/mL overnight at room temperature. The cleavage solution was then evaporated, and the cleaved peptide was dissolved in ACN: H_2O (4:1) and subject to MALDI-TOF for MS/MS analysis.

4.2. *Synthesis of cyclic γ-AApeptides*

The FITC-labeled hits were resynthesized on the Rink Amide resin[2]. Briefly, the Fmoc-dLys (Dde)-OH was first attached to the Rink amide resin. The Fmoc protection group was then removed, followed by the desired building blocks needed for the sequence synthesis. After the γ-AApeptides were cyclized, the Dde group was removed and Fmoc-β-Ala was added, the Fmoc protection group was then removed and FITC (2 equiv.) and DIPEA (6 equiv.) in DMF were added to the resin and shaken for 12 h at room temperature. The FITC labeled cyclic γ-AApeptides was cleaved by 1:1 (*v*/*v*) DCM/TFA containing 2% triisopropylsilane. The crude was purified by the Waters HPLC system.

M-3-1-F: MS: calcd. For $C_{102}H_{120}N_{16}NaO_{16}S_2^+$ $[M+Na]^+$: 1913.2872; MALDI-TOF found: *m*/*z* 1913.3544.

M-3-2-F: MS: calcd. For $C_{103}H_{126}N_{15}O_{18}S_2^+$ $[M+H]^+$: 1926.3475; MALDI-TOF found: *m*/*z* 1926.4503.

M-3-3-F: MS: calcd. For $C_{101}H_{127}N_{17}NaO_{16}S_2^+$ $[M+Na]^+$: 1922.3392; MALDI-TOF found: *m*/*z* 1922.3264.

M-3-4-F: MS: calcd. For $C_{105}H_{124}N_{15}O_{16}S_2^+$ $[M+H]^+$: 1916.3555; MALDI-TOF found: *m*/*z* 1916.3585.

M-3-5-F: MS: calcd. For $C_{96}H_{126}N_{16}NaO_{18}S_2^+$ $[M+Na]^+$: 1879.2672; MALDI-TOF found: *m*/*z* 1878.5530.

M-3-6-F: MS: calcd. For $C_{107}H_{128}N_{15}O_{20}S_2^+$ $[M+H]^+$: 2008.4055; MALDI-TOF found: *m*/*z* 2008.4491.

The synthesis of M-3-6 was conducted on the Rink Amide resin with general solid phrase synthesis. After the γ-AApeptides were cyclized, the compound was cleaved by 1:1 (*v*/*v*) DCM/TFA containing 2% triisopropylsilane and purified by the Waters HPLC system.

M-3-6: MS: calcd. For $C_{77}H_{99}N_{11}NaO_{13}S^+$ $[M+Na]^+$: 1441.7522; MALDI-TOF found: *m*/*z* 1441.2733.

The synthesis of M-3-6-N_3 was conducted on the Rink Amide resin. Briefly, the Fmoc-Lys (Dde)-OH was first attached to the Rink amide resin. The Fmoc protection group was then removed, followed by the desired building blocks needed for the sequence synthesis. After the γ-AApeptides were cyclized, the Dde group was removed and FmocNH-PEG_2-CH_2CO_2H was added, the Fmoc protection group was then removed and 2-azidoacetic acid was added to the resin and shaken for 3 h at room temperature. The FITC labeled cyclic γ-AApeptides was cleaved by 1:1 (*v*/*v*) DCM/TFA containing 2% triisopropylsilane. The crude was purified by the Waters HPLC system.

M-3-6-N_3: MS: calcd. For $C_{91}H_{124}N_{17}O_{18}S^+$ $[M+Na]^+$: 1774.9025; MALDI-TOF found: *m*/*z* 1775.6213.

For the synthesis of M-3-6-D (Supporting Information Scheme S2).

M-3-6-N_3 (10 mg, 0.0056 mmol) and linker (0.95 mg, 0.0026 mmol) was dissolved in DMSO (1 mL), then $CuSO_4 5H_2O$ (1.4 mg, 0.0056 mmol, dissolved in 100 μL DI water) and sodium ascorbate (2.2 mg, 0.0112 mmol, dissolved in 100 μL DI water) were added respectively. The mixture was stirred at room temperature overnight and purified by the Waters HPLC system.

M-3-6-D: HRMS (ESI): calcd. For $C_{202}H_{270}N_{36}O_{41}S_2$: 3919.9258; found: 1308.3184 $[M+3H]^{3+}$, 981.4900 $[M+4H]^{4+}$.

4.3. Fluorescence polarization assay

The FP experiment was performed by incubating 50 nmol/L FITC labeled AApeptides with HER2 (0−2 μmol/L) in PBS. Dissociation constants (K_d) was determined by plotting the fluorescence anisotropy values as a function of protein concentration, and the plots were fitted to Eq. (1):

$$y = \text{FPmin}+(\text{FPmax}-\text{FPmin}) \times (K_D + \text{Lst} + x\text{-sqrt}((K_D + \text{Lst} + x)\hat{}2-4^*\text{Lst}^*x))/(2^*\text{Lst}) \quad (1)$$

where Lst is the concentration of the AApeptides and the *x* stands for the concentration of the protein. The experiments were conducted in triplicates and repeated for three times.

4.4. Surface plasmon resonance assay

Binding kinetics of M-3-6 or M-3-6-D to HER2 was measured by surface plasmon resonance (OpenSPR, Nicoyalife). After HER2 was covalently coupled to the carboxyl sensor chips (Nicoyalife), M-3-6 or M-3-6-D in PBS running buffer (pH 7.4) was slowly flowed over the sensor chip for 5 min to allow interaction. The running buffer was then allowed to flow for 10 min to collect the dissociation data. After subtracting the background, the signal response *vs*. time curve was obtained, binding kinetic parameters were obtained by fitting the curve to a one-to-one binding model using Trace-Drawer (Nicoyalife) software.

4.5. Enzymatic stability assay

Cyclic γ-AApeptides M-3-6-D (0.1 mg/mL) were incubated with 0.1 mg/mL protease in 100 mmol/L ammonium bicarbonate buffer (pH 7.8) at 37 °C for 24 h. Then, the reaction mixtures were concentrated in a speed vacuum to remove water and ammonium bicarbonate. The resulting residues were re-dissolved in H_2O/MeCN and analyzed on a Waters analytical HPLC system.

4.6. Cell cultures and inhibition of EGF-induced cell proliferation

SKBR3 cells were cultured in McCoy's 5A Medium (Gibco) medium containing 10% fetal bovine serum and 1% penicillin/streptomycin in an atmosphere of 5% CO_2 at 37 °C.

SKBR3 cells in good condition were seeded into a 96-well plate at a concentration of 1×10^3 cells/well in 100 μL of complete growth medium. After 24 h of attachment at 37 °C and 5% CO_2, medium was replaced by fresh serum reduced McCoy's 5A Medium and cell were serum-starved overnight. Then serum-reduced EGF (100 ng/mL) McCoy's 5A Medium in the presence of different concentration of M-3-6 and M-3-6-D was added to the cells in hexaplicate. After 72 h, the CCK-8 reagents were added according to the manufacturer's recommendations.

4.7. Western blot assay

SKBR3 cells were seeded into a 6-well plate at a concentration of 1×10^5 cells/well. After 12 h attachment at 37 °C and 5% CO_2, the cells were starved overnight in serum-reduced McCoy's 5A Medium followed by treatment with different concentration of M-3-6 or M-3-6-D for 4 h, and then washed with ice-cold PBS and resuspended in ice-cold RIPA buffer supplemented with Halt Protease and Phosphatase Inhibitor Cocktail. Subsequently, the cells were incubated on ice for 10 min and centrifuged at 14,000×*g* at 4 °C for 10 min. An equal amount of protein was run on 4%−12% Bis-Tris gels, transferred to polyvinylidene difluoride membranes (Millipore) and Western blotted with anti-phosphorylated HER2, anti-phosphorylated AKT, anti-phosphorylated ERK and GAPDH. The experiments were conducted in triplicates and repeated for three times.

4.8. Antitumor studies in nude mice

Male BALB/c nude mice, 4−6 weeks old, were provided by the Shanghai Bikai Experimental Animal Center, with the license number SCXK (Hu) 2008-0016, and maintained under specific-pathogen-free conditions. All animal protocols were approved by the Institutional Animal Use and Care Committee. All the experiments and animal care were approved by Shanghai Medical Experimental Animal Care Commission and in accordance with the Provision and General Recommendation of Chinese Experimental Animals Administration Legislation.

SKBR3 cells were harvested, resuspended in PBS, and injected subcutaneously into 4−6 weeks old Male BALB/c nude mice. When the tumors reach an average size of 100 mm^3, the mice were then randomized divided into four treatment groups: control (PBS), M-3-6 (8 mg/kg), M-3-6 (32 mg/kg), M-3-6-D (8 mg/kg) and trastuzumab (8 mg/kg). Mice were injected through the intraperitoneal every two days for seven injections. 12 days after injection, the mice in each group were killed, and the tumors were removed for examination. The tumor volumes were determined by measuring length (*l*) and width (*w*) and calculating volume as Eq. (2):

$$V = lw^2/2 \quad (2)$$

For the immunohistochemical analysis, the hydrated paraffin section was incubated in a blocking solution (10% donkey serum +5% nonfat dry milk +4% BSA +0.1% Triton X-100) for 10 min, and then incubated at 4 °C overnight with anti-P-HER2, P-AKT,

P-ERK. After washing with PBS, the sections were incubated with diluted (1:200) biotinylated secondary antibody for 30 min. Subsequently, the sections were washed again in PBS and incubated for 30 min with the preformed avidin-horseradish peroxidase macromolecular complex. Development of peroxidase reaction was achieved by incubation in 0.01% 3,3-diaminobenzidine tetrahydrochloride (DAB) in PBS containing 0.01% hydrogen peroxide for approximately 5 min at room temperature. Sections were then washed thoroughly in tap water, counterstained in haematoxylin, dehydrated in absolute alcohol, cleared in xylene and mounted in synthetic resin for microscopic examination.

Acknowledgments

This work was supported by USF start-up fund (Jianfeng Cai) and supported by the National Natural Science Foundation of China (Qi Li, 81520108031, 81573764, 81774095), a Municipal Human Resources Development Program for Outstanding Leaders in Medical Disciplines in Shanghai (Qi Li, 2017BR031, China). Three-years Plan for the Development of T. C. M (ZY (2018−2020)-CCCX-2003-03, China).

Author contributions

Mengmeng Zheng, Chunpu Li and Mi Zhou. conducted most of experiments and performed data analysis; Mengmeng Zheng wrote the manuscript draft; Ru Jia helped to obtain *in vivo* data; Fengyu She obtained MALDI MS/MS data; Lulu Wei helped to for compound preparation and purification; Feng Cheng, Qi Li, Yan Wang and Jianfeng Cai. discussed and analyzed the data; Jianfeng Cai conceived the idea and directed the experiment.

Conflicts of interest

The authors declare no competing interests.

Appendix A. Supporting information

Supporting information to this article can be found online at https://doi.org/10.1016/j.apsb.2021.04.016.

References

1. Hynes NE, Lane HA. ERBB receptors and cancer: the complexity of targeted inhibitors. *Nat Rev Cancer* 2005;**5**:341−54.
2. Petrelli F, Tomasello G, Barni S, Lonati V, Passalacqua R, Ghidini M. Clinical and pathological characterization of HER2 mutations in human breast cancer: a systematic review of the literature. *Breast Cancer Res Treat* 2017;**166**:339−49.
3. King C, Kraus M, Aaronson S. Amplification of a novel v-erbB-related gene in a human mammary carcinoma. *Science* 1985;**229**: 974−6.
4. Arteaga Carlos L, Engelman Jeffrey A. ERBB receptors: from oncogene discovery to basic science to mechanism-based cancer therapeutics. *Cancer Cell* 2014;**25**:282−303.
5. Burstein HJ. The distinctive nature of HER2-positive breast cancers. *N Engl J Med* 2005;**353**:1652−4.
6. Vogel CL, Cobleigh MA, Tripathy D, Gutheil JC, Harris LN, Fehrenbacher L, et al. Efficacy and safety of trastuzumab as a single agent in first-line treatment of HER2-overexpressing metastatic breast cancer. *J Clin Oncol* 2002;**20**:719−26.
7. Capelan M, Pugliano L, De Azambuja E, Bozovic I, Saini KS, Sotiriou C, et al. Pertuzumab: new hope for patients with HER2-positive breast cancer. *Ann Oncol* 2012;**24**:273−82.
8. Moy B, Goss PE. Lapatinib: current status and future directions in breast cancer. *Oncol* 2006;**11**:1047−57.
9. Chan A. Neratinib in HER-2-positive breast cancer: results to date and clinical usefulness. *Ther Adv Med Oncol* 2016;**8**:339−50.
10. Garrett JT, Arteaga CL. Resistance to HER2-directed antibodies and tyrosine kinase inhibitors. *Cancer Biol Ther* 2011;**11**:793−800.
11. Xu ZQ, Zhang Y, Li N, Liu PJ, Gao L, Gao X, et al. Efficacy and safety of lapatinib and trastuzumab for HER2-positive breast cancer: a systematic review and meta-analysis of randomised controlled trials. *BMJ Open* 2017;**7**:e013053.
12. Scheuer W, Friess T, Burtscher H, Bossenmaier B, Endl J, Hasmann M. Strongly enhanced antitumor activity of trastuzumab and pertuzumab combination treatment on HER2-positive human xenograft tumor models. *Cancer Res* 2009;**69**:9330−6.
13. Baselga J, Cortés J, Kim SB, Im SA, Hegg R, Im YH, et al. Pertuzumab plus trastuzumab plus docetaxel for metastatic breast cancer. *N Engl J Med* 2011;**366**:109−19.
14. Swain SM, Baselga J, Kim SB, Ro J, Semiglazov V, Campone M, et al. Pertuzumab, trastuzumab, and docetaxel in HER2-positive metastatic breast cancer. *N Engl J Med* 2015;**372**:724−34.
15. Shi Y, Teng P, Sang P, She F, Wei L, Cai J. γ-AApeptides: design, structure, and applications. *Acc Chem Res* 2016;**49**:428−41.
16. Teng P, Shi Y, Sang P, Cai J. γ-AApeptides as a new class of peptidomimetics. *Chem Eur J* 2016;**22**:5458−66.
17. Teng P, Ma N, Cerrato DC, She F, Odom T, Wang X, et al. Right-handed helical foldamers consisting of *de novo* d-AApeptides. *J Am Chem Soc* 2017;**139**:7363−9.
18. She F, Teng P, Peguero-Tejada A, Wang M, Ma N, Odom T, et al. *De novo* left-handed synthetic peptidomimetic foldamers. *Angew Chem Int Ed* 2018;**57**:9916−20.
19. Teng P, Niu Z, She F, Zhou M, Sang P, Gray GM, et al. Hydrogen-bonding-driven 3D supramolecular assembly of peptidomimetic zipper. *J Am Chem Soc* 2018;**140**:5661−5.
20. Teng P, Gray GM, Zheng M, Singh S, Li X, Wojtas L, et al. Orthogonal halogen-bonding-driven 3D supramolecular assembly of right-handed synthetic helical peptides. *Angew Chem Int Ed* 2019;**58**: 7778−82.
21. Sang P, Zhang M, Shi Y, Li C, Abdulkadir S, Li Q, et al. Inhibition of β-catenin/B cell lymphoma 9 protein−protein interaction using α-helix-mimicking sulfono-γ-AApeptide inhibitors. *Proc Natl Acad Sci U S A* 2019;**116**:10757−62.
22. Shi Y, Challa S, Sang P, She F, Li C, Gray GM, et al. One-bead-two-compound thioether bridged macrocyclic γ-AApeptide screening library against EphA2. *J Med Chem* 2017;**60**:9290−8.
23. Shi Y, Parag S, Patel R, Lui A, Murr M, Cai J, et al. Stabilization of lncRNA GAS5 by a small molecule and its implications in diabetic adipocytes. *Cell Chem Biol* 2019;**26**:319−330.e6.
24. Yan H, Zhou M, Bhattarai U, Song Y, Zheng M, Cai J, et al. Cyclic peptidomimetics as inhibitor for miR-155 Biogenesis. *Mol Pharm* 2019;**16**:914−20.
25. Handl HL, Sankaranarayanan R, Josan JS, Vagner J, Mash EA, Gillies RJ, et al. Synthesis and evaluation of bivalent NDP-α-MSH(7) peptide ligands for binding to the human melanocortin receptor 4 (hMC4R). *Bioconjugate Chem* 2007;**18**:1101−9.
26. Udugamasooriya DG, Dineen SP, Brekken RA, Kodadek T. A peptoid "antibody surrogate" that antagonizes VEGF receptor 2 activity. *J Am Chem Soc* 2008;**130**:5744−52.
27. Kodadek T. Development of antibody surrogates for the treatment of cancers and autoimmune disease. *Curr Opin Chem Biol* 2010;**14**: 721−7.
28. Sarkar M, Liu Y, Morimoto J, Peng H, Aquino C, Rader C, et al. Recognition of antigen-specific B-cell receptors from chronic lymphocytic leukemia patients by synthetic antigen surrogates. *Chem Biol* 2014;**21**:1670−9.

29. Sarkar M, Liu Y, Qi J, Peng H, Morimoto J, Rader C, et al. Targeting stereotyped B cell receptors from chronic lymphocytic leukemia patients with synthetic antigen surrogates. *J Biol Chem* 2016;**291**:7558−70.
30. Garrett TPJ, McKern NM, Lou M, Elleman TC, Adams TE, Lovrecz GO, et al. The crystal structure of a truncated ErbB2 ectodomain reveals an active conformation, poised to interact with other ErbB receptors. *Mol Cell* 2003;**11**:495−505.
31. Yarden Y, Pines G. The ERBB network: at last, cancer therapy meets systems biology. *Nat Rev Cancer* 2012;**12**:553−63.
32. Larionov AA. Current therapies for human epidermal growth factor receptor 2-positive metastatic breast cancer patients. *Front Oncol* 2018;**8**:89.
33. Ritter CA, Perez-Torres M, Rinehart C, Guix M, Dugger T, Engelman JA, et al. Human breast cancer cells selected for resistance to trastuzumab *in vivo* overexpress epidermal growth factor receptor and ErbB ligands and remain dependent on the ErbB receptor network. *Clin Cancer Res* 2007;**13**:4909−19.
34. Holliday DL, Speirs V. Choosing the right cell line for breast cancer research. *Breast Cancer Res* 2011;**13**:215.